Model-free vibration control based on a virtual controlled object considering actuator uncertainty

Ansei Yonezawa[1], Itsuro Kajiwara[1] and Heisei Yonezawa[1]

Ansei Yonezawa[1]

E-mail: ansei316@eis.hokudai.ac.jp

Itsuro Kajiwara[1]

E-mail: ikajiwara@eng.hokudai.ac.jp

Heisei Yonezawa[1]

E-mail: heisei620@eis.hokudai.ac.jp

[1]Division of Human Mechanical Systems and Design, Hokkaido University

N13, W8, Kita-ku, Sapporo, Hokkaido, 060-8628, Japan

Corresponding author

Itsuro Kajiwara

Division of Human Mechanical Systems and Design, Hokkaido University

N13, W8, Kita-ku, Sapporo, Hokkaido, 060-8628, Japan

Email: ikajiwara@eng.hokudai.ac.jp

Tel: +81 11 706 6390, Fax: +81 11 706 6390

Abstract

The purpose of this research is to construct a simple and practical controller design method, considering the actuator's parameter uncertainty, without using a model of the controlled objects. In this method, a controller is designed with an actuator model including a single-degree-of-freedom (SDOF) virtual structure inserted between the actuator and the controlled object, resulting in a model-free controller design. Furthermore, an H_∞ control problem is defined so that the actuator's parameter uncertainty is compensated by satisfying a robust stability condition. Because the actuator model including the virtual controlled object is a simple low-order system, and the actuator's parameter uncertainty is considered, a controller with high robustness to the actuator's parameter uncertainty can be designed based on traditional model-based control theory. The effectiveness of the proposed method is verified by both simulations and experiments.

Keywords

Model-free control, Active vibration control, Virtual controlled object, H_∞ control, Proof-mass actuator, Actuator uncertainty, Robust control

1.Introduction

To successfully downsize, lighten, and improve the performance of mechanical systems, vibration control is necessary. Active vibration control, which has strong vibration-reduction effect, has been widely studied in recent years (Parameswaran et al, 2013; Parameswaran & Gangadharan, 2015; Kant & Parameswaran, 2018). However, design of an active vibration controller is generally based on a mathematical model of the controlled object. Therefore, design of the controller is associated with an enormous burden on the designer, as well as a cost increase, due to the need to individually model each controlled object. In addition, because control performance and stability greatly depend on model accuracy, controllers designed based on models are vulnerable to modeling error and model changes that always occur in real systems.

Therefore, in recent years, research effort has focused on model-free active control systems that do not use a controlled object model. These studies have proposed a semi-active vibration control system that took into account physical insights about the dynamics of semi-active suspension (Swevers et al., 2007), examined an adaptive attitude control system for flexible spacecraft based on the Euler-Lagrange method (Wei et al., 2018), and compared a model-free controlled system with a traditional model-based controlled system in a flexible-link robot (Rigatos, 2009). An earlier study proposed an

active noise control system that considered the frequency characteristics of the disturbance (Meurers et al., 2003). There are several unique methods as such control systems.

Real-time tuning methods based on the simultaneous perturbation stochastic approximation (SPSA) have been proposed (Zhou et al., 2008; Ishizuka and Kajiwara, 2015). Using the SPSA, an adaptive vibration control method for tuning the poles of the H_∞ controller, adjusting for variations in the controlled object's characteristics, has been investigated (Kajiwara et al., 2018). However, real-time optimization is often difficult to implement due to the high calculation cost.

Introducing neural networks (NNs) into a control system is an effective way to achieve model-free control. Accordingly, several studies have been conducted on model-free control using NNs (Yildirim, 2004; Madan, 2005; Yousefi et al., 2008; Zhang et al., 2017). One group proposed vibration control of a flexible cantilever using a neurocontroller constructed by emulator NNs has been proposed (Abdeljaber et al., 2016). Another study conducted both system identification and vibration control with an active mass-damper created by NNs (Yang et al., 2006). In general, however, approaches based on NNs require a huge amount of training data to learn vibration control, inflicting a heavy burden on the designer. Additionally, it takes a great deal of time to learn and optimize to

a sufficient degree to achieve satisfactory performance.

The fuzzy control method involves if/then–type control rules based on the fuzzy set expressed empirical knowledge and plant information. Thus, a mathematical model of the plant is not always necessary in order to design it; consequently, it can be a construct model-free control system. There are many examples of adaptation to real systems, e.g., combination with a PI/PID controller for compensation of nonlinear restoring forces in vibration control of a building structure (Thenozhi and Yu, 2015). This method was used for tuning of mass damper by the fuzzy logic in vibration control of a building structure (Edalath et al., 2013). Moreover, fuzzy modal feedback has been applied to flexible structures (Malhis et al., 2005). Nevertheless, in general, there are not yet methodical approaches for determining the control rules or membership functions; consequently, these depend in a large part on the designer's experience and intuition.

Sliding mode control (SMC) is often applied to model-free control systems. For example, model-free SMC was achieved by setting an appropriate smoothing function to control a rotary inverted pendulum (Yiğit, 2017); NN tuning based on SMC has been applied to control of an overhead crane (Lee et al., 2014); an active suspension system has been controlled by SMC (Wang et al., 2019); and vibration suppression of flexible cantilever plate has been studied (Parameswaran et al., 2015; Parameswaran et al., 2015).

However, the chattering caused by switching the control input of SMC becomes a major problem when this approach is applied to a mechanical system. Parameter tuning by trial and error method is essential in order to compensate for chattering.

Collectively, the studies described above demonstrate that there are very few simple and practical model-free active vibration control approaches that place low burdens on designers. In a previous study, an approach that could achieve this goal was suggested. Specifically, designing a controller using a model of the actuator and a model of the virtual structure represented by a single-degree-of-freedom (SDOF) system was proposed as a model-free vibration control system (Yonezawa et al., 2019; Yonezawa et al., 2020). The model of the actuator described in that work must be accurate, including the parameter values. In general, however, actuator parameters have uncertainties due to individual differences in manufacture and degradation over long-term use, and these uncertainties adversely affect control performance and stability. Accordingly, the model-free control system must be robust against an actuator's parameter uncertainty.

In this study, a model-free active vibration control approach that has a simple design process, decreases the burden on designers, and guarantees robustness against uncertainty about the parameters of the actuator is proposed. This method achieves model-free design using the virtual structure that was proposed in the previous studies,

and quantitatively evaluates the uncertainty of the actuator parameters using the H_∞ norm. Specifically, by inserting the virtual structure defined as the SDOF system between the actual controlled object and the actuator, and setting the appropriate parameters based on consideration of the frequency transfer characteristics, a model-free control system was constructed. Next, the uncertainty of the actuator parameters was modeled for the configured control system, and it was showed that the configured control system with the uncertainty can be described by the plant set with feedback-type fluctuations. Then, based on H_∞ control theory, a typical robust control theory, a controller that can compensate for the uncertainty in actuator parameters and provide robust stabilization was designed. Thus, the controller was designed without using any parameters of the controlled object, compensating for the parameter uncertainty of the actuator. By designing the controller using a virtual structure model defined as an SDOF system, model-free design could be easily achieved with just a few design variables. After the introduction of the virtual structure, the controller was designed in exactly the same way as a traditional model-based controller. Therefore, it was possible to compensate for uncertainties in actuator parameters based on mature traditional H_∞ control theory. Finally, the effectiveness of the proposed method was confirmed by both simulations and experiments. The numerical studies were conducted for a simple SDOF controlled object

to verify robustness against uncertainty in the actuator parameters. In addition, to demonstrate the applicability of the proposed method to actual mechanical structure, the experimental verifications used a cantilever plate as a controlled object of a continuum structure. Both simulations and experimental results validated the effectiveness of the proposed method.

2. System for designing a model-free controller

2.1. Actuator

Figure 1 shows the actuator used in this paper. This is a proof–mass actuator installed on the surface of target structures. Specifically, the mass of the movable part consisting of the coil applies an excitation force in a direction normal to the contact surface and suppresses the vibration of the controlled object. The excitation force is proportional to the current value in the actuator circuit, which is determined by the value indicated by the controller. Thus, the proof–mass type actuator can be modeled as a single-degree-of-freedom (SDOF) system.

2.2. Control method for model-free controller design

In this study, model-free active vibration control is achieved by inserting a virtual controlled object between the model of the actuator and the model of the actual controlled object (Yonezawa et al., 2019; Yonezawa et al., 2020). Figure 2(a) shows the model of the actual structure. m, k, and c represent mass, stiffness, and damping. Subscript 0 indicates the actuator model, and subscript 1 indicates the actual controlled object. The structure of the controlled object is not clearly defined, but is instead an arbitrary structure.

Figure 2(b) shows a model in which a virtual structure is inserted between the actuator model and the controlled object model to design a model-free controller. Subscript v indicates the virtual structure. The aim is to suppress the vibration of the controlled object (displacement x_1) indirectly by considering the virtual structure as the actual controlled object, and then controlling displacement x_v of the virtual structure. Then, the controller is designed based on the traditional model-based control theory for a two-degree-of-freedom (2DOF) system consisting of the actuator and the virtual structure.

Table 1. Parameters for the control system design

Properties	Value	Unit
m_0	0.2013	Kg
k_0	3518	N/m
c_0	1.186	Ns/m
m_v	10^{-5}	Kg
k_v	7.0×10^5	N/m
c_v	0.0	Ns/m

The equations of motion of the actuator and the virtual structure can be written as

$$m_0\ddot{x}_0 + c_0(\dot{x}_0 - \dot{x}_v) + k_0(x_0 - x_v) = u \tag{1}$$

$$m_v\ddot{x}_v + c_v(\dot{x}_v - \dot{x}_1) + k_v(x_v - x_1) + c_0(\dot{x}_v - \dot{x}_0) + k_0(x_v - x_0) = -u \tag{2}$$

Then, equations (1) and (2) are Laplace transformed with the all initial conditions set to zero, and T_{xvx1}, which represents the transfer characteristic from x_1 to x_v, is written in equation (3). Here, s is the Laplace variable, and the functions after the transformation are expressed as capital letters.

$$T_{xvx1} = \frac{X_v(s)}{X_1(s)} = \frac{(m_0 s^2 + c_0 s + k_0)(c_v s + k_v)}{\{m_v s^2 + (c_0 + c_v)s + (k_0 + k_v)\}(m_0 s^2 + c_0 s + k_0) - (c_0 s + k_0)^2} \quad (3)$$

The parameters of the virtual structure are the design variables. The purpose of this study is to suppress the vibration of the controlled object when it vibrates at a certain frequency ($s = j\omega$) in the system shown in Figure 2(b). That is, for T_{xvx1} in equation (3), s takes a certain non-zero value ($s = j\omega \neq 0$) corresponding to the actual vibrating state of the controlled object in the controlled frequency band. Here, the vibration of the virtual structure can be expressed as $X_v = T_{xvx1} \times X_1$. Therefore, because x_v becomes the same as x_1 if T_{xvx1} converges to 1, it is possible to indirectly suppress the vibration x_1 of the actual controlled object by suppressing the vibration x_v of the virtual structure. In equation (3), the transfer characteristic T_{xvx1} converges to 1 for all s ($\neq 0$) in the frequency band where vibration control is performed when the virtual structure is designed such that $k_v \to \infty$ and $m_v = 0$.

On the other hand, k_v must be defined as a finite value, and m_v must not be defined as 0, because the controller is derived by numerical calculation. For that reason, the aim is to approximately establish the following transfer characteristic:

$$T_{xvx1} \approx 1 \tag{4}$$

When k_v has a sufficiently large finite positive value, m_v has a sufficiently small finite positive value, and c_v is 0, the transfer characteristic of equation (4) is satisfied, and indirect vibration control can be achieved. Table 1 shows the parameters of the actuator and the virtual structure.

In the system shown in Figure 2(b), a controller is designed by using only the equations (1) and (2) of motions of the actuator and the virtual structure in order to achieve a model-free design for the controlled object. Here, the system composed of (1) and (2) is regarded as the 2DOF system consisting only of the actuator and the virtual structure. Then, a state equation of the 2DOF system can be derived from equations (1) and (2) by defining its state variable vector, which is composed only of their vibrations x_0 $(\dot{x}_0)$ and x_v $(\dot{x}_v)$. In particular, in equations (1) and (2), the force $c_v\dot{x}_1 + k_v x_1$, which is caused by the vibration of the actual controlled object, can be regarded as an exciting force exerted from the outside to the 2DOF system. Consequently, in equations (1) and (2), disturbance w is defined as

$$w = c_v\dot{x}_1 + k_v x_1 \tag{5}$$

Then, the state equation of 2DOF system can be derived as shown below.

$$\dot{x}_{va} = A_{va}x_{va} + B_{va1}w + B_{va2}u \tag{6}$$

$$x_{va} = [x_v \quad x_0 \quad \dot{x}_v \quad \dot{x}_0]^T \tag{7}$$

$$A_{va} = \begin{bmatrix} 0 & 0 & 1 & 0 \\ 0 & 0 & 0 & 1 \\ -\dfrac{k_0 + k_v}{m_v} & \dfrac{k_0}{m_v} & -\dfrac{c_0 + c_v}{m_v} & \dfrac{c_0}{m_v} \\ \dfrac{k_0}{m_0} & -\dfrac{k_0}{m_0} & \dfrac{c_0}{m_0} & -\dfrac{c_0}{m_0} \end{bmatrix}, B_{va1} = \begin{bmatrix} 0 \\ 0 \\ \dfrac{1}{m_v} \\ 0 \end{bmatrix}, B_{va2} = \begin{bmatrix} 0 \\ 0 \\ -\dfrac{1}{m_v} \\ \dfrac{1}{m_0} \end{bmatrix} \tag{8}$$

That state equation does not include any parameters of the actual controlled object. Therefore, model-free vibration control is achieved by designing a controller for state equation (6), which regards the virtual structure as the controlled object.

Vibration control is performed by feeding back the vibration response of the virtual structure as observed output in the feedback control system, as shown above. On the other hand, the virtual structure does not exist in the actual system. Hence, from equation (4), vibration of the actual controlled object x_1, which is almost the same as x_v, is used as observed output in actual feedback control.

2.3. Design of virtual controlled object

Equation (4) holds for a limited frequency band because the parameters of the virtual structure cannot be defined as $k_v \to \infty$ and $m_v = 0$. Hence, it is necessary to design the virtual structure such that equation (4) holds in the control frequency band where vibration is suppressed. The design condition (9) for a virtual structure was derived in the previous study (Yonezawa et al., 2020). In this study, the parameters of the virtual structure are determined based on equation (9). In equation (9), the lower-limit and upper-limit frequencies of the vibration control band are defined as Ω_1^{cont} and Ω_2^{cont} ($\Omega_2^{cont} > \Omega_1^{cont} \geq \sqrt{\frac{k_0}{m_0}}$), respectively.

$$\left\{\left(\frac{(\Omega_k^{cont})^2}{k_0} - \frac{1}{m_0}\right)k_v + (\Omega_k^{cont})^2\right\}\frac{1}{m_v} > \left(\frac{(\Omega_k^{cont})^2}{k_0} - \frac{1}{m_0}\right)(\Omega_k^{cont})^2, (k = 1, 2) \tag{9}$$

Figure 3 shows the Bode diagram of the frequency characteristic of $T_{xvx1}(s)$ treated in this study. In $f \in (f_1 \cong 20.6\text{Hz},\ f_2 \cong 4.03 \times 10^4\text{Hz})$ including the control frequency band, equation (4) holds because the gain can be regarded as 1 and the phase can be regarded as 0° .

3. Controller design

3.1. Modeling of actuator's parameter uncertainty

In this study, the model-free vibration control system is constructed when equation (6) includes the actuator's parameter uncertainty. In that case, the stiffness and damping of the actuator are regarded as uncertain. The parameters of the actuator with uncertainty can be written as

$$\begin{aligned} k_{0m} &= k_{0n} + \Delta_k k_e, \qquad -1 \leq \Delta_k \leq 1 \\ c_{0m} &= c_{0n} + \Delta_c c_e, \qquad -1 \leq \Delta_c \leq 1 \end{aligned} \tag{10}$$

k_{0m} and c_{0m} are the actual values of k_0 and c_0, which include uncertainties with values shown in Table 1. k_{0n} and c_{0n} are nominal values, which are the same as the values of k_0 and c_0 shown in Table 1. Δ_k and Δ_c are normalized fluctuations. k_e and c_e are the maximum amounts of uncertainties of the parameters to be compensated and are known at the time of design. Then, the actual stiffness k_{0m} and the actual damping c_{0m} can be expressed as uncertain values, which are nominal values k_{0n} and c_{0n} with maximum fluctuations $\pm k_e$ and $\pm c_e$. In addition, both controlled output and observed output are defined as acceleration of the virtual structure $\ddot{x}_v$. Thus, the transfer function

$\tilde{P}(s)$ from control input to controlled output can be expressed as equation (11) by substituting k_{0m} and c_{0m} for k_0 and c_0 and defining c_v as 0.

$$\tilde{P}(s) = \frac{s^2 X_v}{U} = \frac{P(s)}{1 + \Delta W(s)} \tag{11}$$

$$P(s) = \frac{-m_0 s^4}{m_0 m_v s^4 + (m_0 + m_v) c_{0n} s^3 + \{(m_0 + m_v) k_{0n} + m_0 k_v\} s^2 + c_{0n} k_v s + k_{0n} k_v} \tag{12}$$

$$W(s) = \begin{bmatrix} W_1(s) \\ W_2(s) \end{bmatrix} = \begin{bmatrix} \dfrac{(m_0 + m_v) c_e s^3 + k_v c_e s}{m_0 m_v s^4 + (m_0 + m_v) c_{0n} s^3 + \{(m_0 + m_v) k_{0n} + m_0 k_v\} s^2 + c_{0n} k_v s + k_{0n} k_v} \\ \dfrac{(m_0 + m_v) k_e s^2 + k_v k_e}{m_0 m_v s^4 + (m_0 + m_v) c_{0n} s^3 + \{(m_0 + m_v) k_{0n} + m_0 k_v\} s^2 + c_{0n} k_v s + k_{0n} k_v} \end{bmatrix} \tag{13}$$

$$\Delta = [\Delta_c \quad \Delta_k], \quad \|\Delta\|_\infty \leq 1 \tag{14}$$

$P(s)$ is the transfer function from control input to controlled output when the actuator is nominal. $W(s)$ is the weighting function expressing the fluctuation of the transfer function caused by actuator uncertainty. Δ is the normalized fluctuation matrix. From equation (11), the control system with actuator uncertainty can be expressed as the plant set with the feedback-type plant fluctuation shown in Figure 4(a).

3.2. H_∞ controller design

Next, a model-free controller considering actuator's uncertainty is designed for the

plant set with feedback-type plant fluctuation (Figure 4(a)) based on H_∞ control theory. Figure 4(b) shows the generalized plant for considering the actuator's uncertainty based on the Small-gain theorem for the constructed plant set (Zbou et al., 1996). The constant weights Q and R shown in Figure 4(b) are determined as 3.2×10^{-1} and 1.4×10^{4}, respectively. Specifically, they were determined by actually conducting the simulations and the experiments and confirming the results demonstrated later. Some adjustments by trial and error were also involved.

Equations (15)–(18) show the formulations of the controlled object and the controlled variables of Figure 4(b).

$$P : \begin{cases} \dot{x}_P = A_P x_P + B_{P1} w + B_{P2} u \\ y = C_P x_P + D_{P1} w + D_{P2} u \end{cases} \tag{15}$$

$$W_1 : \begin{cases} \dot{x}_{e1} = A_{e1} x_{e1} + B_{e1} y' \\ z_{e1} = C_{e1} x_{e1} + D_{e1} y' \end{cases} \tag{16}$$

$$W_2 : \begin{cases} \dot{x}_{e2} = A_{e2} x_{e2} + B_{e2} y' \\ z_{e2} = C_{e2} x_{e2} + D_{e2} y' \end{cases} \tag{17}$$

$$y' = y - w_e \quad z_1 = Q y' \quad z_2 = R u \tag{18}$$

Equation (15) represents the state equation of the 2DOF system consisting of the nominal actuator and the virtual structure when the acceleration $\ddot{x}_v$ of the virtual structure is output. This equation can be obtained by realizing the transfer function (12)

(i.e., transforming the transfer function (12) into its state space representation). Equations (16) and (17) can be obtained by realizing each component of the transfer function vector $W(s)$, which represents the fluctuations of the 2DOF system due to the actuator's uncertainty, shown in equation (13). Equation (18) shows the relationship between each signal shown in Figure 4(b). y' is the acceleration of the virtual structure. z_1 and z_2 are the controlled variables considering each constant weight. w_e represents the effect due to the actuator uncertainty as a disturbance, and can be defined from the Small-gain theorem (Zbou et al., 1996). By H_∞ control theory, for vibration control considering the actuator uncertainty, the controller K is designed such that $\|F_l(G,K)\|_\infty$, which is the H_∞ norm of the closed-loop transfer function $F_l(G,K)$ from w' to z shown in Figure 4(b), is minimized (Zbou et al., 1996). In this study, a linear matrix inequality approach is used to solve the H_∞ control problem. Control System Toolbox and Robust Control Toolbox of MATLAB were used to transform the transfer functions (12) and (13) into their state space representations (15)–(17) and to design the controller.

Below, the design procedure of the model-free controller proposed in this paper is briefly summarized.

1. The controlled frequency band is set.

2. The parameters of the SDOF virtual structure, m_v and k_v, are designed to satisfy equation (9) in the controlled frequency band. Specifically, m_v and k_v should be determined as a sufficiently small positive value and a sufficiently large positive value, respectively.
3. A range of the actuator's parameter uncertainties to be compensated is set using the maximum permissible error amounts, k_e and c_e.
4. The H_∞ controller is designed using the generalized plant described in equations (15)–(18) in exactly the same way as traditional model-based approaches using numerical software such as MATLAB. As a tuning policy, Q should be larger when the control performance is more important, and R should be larger when the control input needs to be limited.

4. Simulation study

4.1. Configuration of the simulation

A simulation study is performed to verify the robustness of the approach proposed in Chapter 3 with respect to uncertainty in the actuator parameters. In the simulation, which is a basic study, the controlled object was the simple SDOF vibration system shown

in Figure 5, making it easier to evaluate the influence of actuator errors. In Figure 5, the mass m_1[kg], stiffness k_1[N/m] and damping c_1[Ns/m] are set as 1.2, 1.0×10^6 and 10.95, respectively (Yonezawa et al., 2019). For the H_∞ controller designed for equations (6)–(8) without considering the uncertainty of the actuator (Controller 1) and the H_∞ controller designed with consideration of the uncertainty of the actuator (Controller 2), the vibration control simulation was conducted by changing the parameter values of the actuator, and the robustness of the proposed Controller 2 was verified. The error range of the actuator to be compensated was $\pm 50\%$. Vibration control performance was evaluated based on the acceleration of the controlled object.

4.2. Control simulation results and discussion

Figure 6 shows the frequency responses of the acceleration from the disturbance to the observed output obtained in the simulation. The blue line is the frequency response without control, the red line is the closed-loop frequency response of Controller 1, and the green line is the closed-loop frequency response of Controller 2. The symbols ErK and ErC indicate that the actual values during the simulation have errors of ErK[%] and ErC[%], respectively, for the normal actuator stiffness and damping shown in Table 1. Table 2 shows the results of vibration suppression for the parameter error of each

actuator shown in Figure 6.

Table 2. Results of vibration control simulations

Parameters of Actuator		Reduction amount [dB]		Reduction efficiency [%]	
ErK [%]	ErC [%]	Controller 1 1st peak (146 Hz)	Controller 2 1st peak (146 Hz)	Controller 1 1st peak (146 Hz)	Controller 2 1st peak (146 Hz)
0	0	−31.3	−31.6	97.3	97.4
50	−50	*unstable*	−31.3	*unstable*	97.3

In Figure 6(a), because the actuator does not include errors, sufficient damping performance is obtained without instability in both Controllers 1 and 2. On the other hand, in Figure 6(b), Controller 2 achieves a stable and sufficient damping effect even though Controller 1 results in instability. This effect is created by the generalized plant designed in Chapter 3 and the H_∞ control problem. From the above, the proposed method of this study added robustness with respect to the uncertainty of the actuator used for the previously described model-free controller (Yonezawa et al., 2019; Yonezawa et al., 2020).

5. Experimental verification

5.1. Configuration of the experimental system

Figure 7 shows the experimental setup. In this study, the principal purpose of the experimental verification was to demonstrate the applicability of the proposed control system to actual mechanical structures. The structure shown in Figure 7(a), a cantilever plate with dimensions 190 mm × 248 mm × 10 mm and made of aluminum, was used as the controlled object. A load cell was installed at position A to apply a disturbance with a shaker and to measure the force. The control input was applied by the actuator attached to position B in Figure 7(a). The observed output was measured by an acceleration sensor attached to position C on the back of the flat plate at the actuator installation position. Figure 7(b) is a closed-loop system, and Figure 7(c) shows an actual experimental setup. The observed output was input to a digital signal processor (DSP). The control input command value calculated by DSP passed through an analog low-pass filter (Order: 4; Type: Butterworth) to prevent spillover, and was then amplified by a current amplifier to drive the actuator. As a disturbance, a 1–1000 Hz linear sweep sinusoidal signal was delivered from the signal generator. The spectrum analyzer measured the frequency response from the disturbance (load cell) to the observed output (acceleration obtained from the sensor). That is, the vibration control performance was evaluated based on the acceleration of the controlled object. The control bandwidth in

this study was set from 50 to 1000 Hz.

To experimentally evaluate robust stability with respect to actuator uncertainty, it is difficult to use multiple actuators with various parameters. Therefore, in this study, the parameters of the actuator model shown in Table 1, defined as nominal during controller design, were altered. When the controller is designed using that actuator model, the situation where parameter errors occur is created equivalently for the unique actuator used in the experiment. The error range of the actuator to be compensated was $\pm 50\%$.

From the above, based on the method shown in Chapter 3, the H_∞ controller was designed using various actuator parameters, and the vibration control experiment was performed on the cantilever plate.

5.2. Experimental results and discussion

Figures 8–12 show the results of the control experiment. These are the frequency responses of the acceleration from the disturbance to the observed output. The blue line in each graph is the frequency response without control, and the red line is the closed-loop frequency response with control. ErK and ErC indicate that the stiffness and damping of the actuator parameters used in the experiment had errors of $ErK[\%]$ and $ErC[\%]$, respectively, with respect to the stiffness and damping of the actuator used

for controller design. Table 3 shows the results of vibration suppression for the parameter error of each actuator shown in Figures 8–12.

Table 3. Results of vibration control experiments

Parameters of Actuator		Reduction amount [dB]		Reduction efficiency [%]	
ErK [%]	ErC [%]	1st peak (114 Hz)	3rd peak (257 Hz)	1st peak (114 Hz)	3rd peak (257 Hz)
0	0	−12.8	−14.1	77.1	80.3
50	50	−13.5	−11.4	78.9	73.1
−50	50	−14.0	−14.8	80.1	81.8
50	−50	−7.9	−6.4	59.7	52.1
−50	−50	−7.5	−6.9	57.8	54.8

As shown in Figures 8–12 and Table 3, sufficient damping effect is obtained for each mode up to 500 Hz in the control frequency band, despite the uncertainty in the actuator parameters. Therefore, the model-free controller designed by the approach proposed in this study has a high damping effect on actual mechanical structures.

In this study, the parameters of each actuator used for controller design in Figures 8–12 are different for the sake of the experiment. However, the constant weights Q and R applied to the acceleration $\ddot{x}_v$ of the virtual structure and the control inputs were those shown in Section 3.2. Therefore, there are better constant weights Q and R for the parameters of each actuator used in the controller design, and it is possible that

performance could be improved by adjusting the parameters.

In the proposed approach, when Q and R need to be adjusted, the prototype controller has to be halted and reprogrammed with new control parameters before deployment. In order to make the proposed approach more practical in the real world, the controller parameters need to be adjusted dynamically as per the changes in the occurring dynamics.

6. Conclusion

In this study, a model-free active vibration control approach considering the uncertainty of actuator parameters was proposed based on an actuator model that included the virtual controlled object, based on H_∞ control theory. The proposed method achieves indirect vibration control without using a model of the actual controlled object by inserting a virtual structure between the actuator modeled in the SDOF system and the actual controlled object. To achieve robustness against modeling error, the uncertainties of the actuator parameters are modeled. This means that a controller design model with actuator uncertainty can be described by a plant set with feedback-type fluctuations. Next, the controller that guarantees robustness against uncertainty of actuator parameters for the derived plant set was designed based on the H_∞ control theory. Finally, the effectiveness of the proposed approach was verified by simulations and experiments. The results confirmed high robustness against actuator parameter error and a sufficient vibration reduction effect in an actual system.

In future extensions of this research, the versatility of this approach will be verified by applying it to other actual mechanical systems. In other future works, the model-free controller is planned to be improved by combining it with an adaptive approach in which the controller parameters are adjusted automatically according to changes in the occurring dynamics.

Declaration of Conflicting Interests

The author(s) declared no potential conflicts of interest with respect to the research, authorship, and/or publication of this article.

Funding

The author(s) disclosed receipt of the following financial support for the research, authorship, and/or publication of this article: We thank the Japan Society for the Promotion of Science for their support under Grants-in-Aid for Scientific Research Programs (Grants-in-Aid for Scientific Research (B), Project No. JP 19H02088).

References

Abdeljaber O, Avci O and Inman DJ (2016) Active vibration control of flexible cantilever plates using piezoelectric materials and artificial neural networks. *Journal of Sound and Vibration*, *363*, 33–53. https://doi.org/10.1016/j.jsv.2015.10.029

Edalath S, Kukreti AR and Cohen K (2013) Enhancement of a tuned mass damper for building structures using fuzzy logic. *Journal of Vibration and Control*.

https://doi.org/10.1177/1077546312449034

Ishizuka S and Kajiwara I (2015) Online adaptive PID control for MIMO systems using simultaneous perturbation stochastic approximation. *Journal of Advanced Mechanical Design, Systems and Manufacturing*, *9*(2), 1–16. https://doi.org/10.1299/jamdsm.2015jamdsm0015

Kajiwara I, Furuya K and Ishizuka S (2018) Experimental verification of a real-time tuning method of a model-based controller by perturbations to its poles. *Mechanical Systems and Signal Processing*, *107*, 396–408. https://doi.org/10.1016/j.ymssp.2018.01.017

Kant M and Parameswaran AP (2018) Modeling of low frequency dynamics of a smart system and its state feedback based active control. *Mechanical Systems and Signal Processing*, 99, 774–789. https://doi.org/10.1016/j.ymssp.2017.07.018

Lee LH, Huang PH, Shih YC, et al. (2014) Parallel neural network combined with sliding mode control in overhead crane control system. *Journal of Vibration and Control*, *20*(5), 749–760. https://doi.org/10.1177/1077546312464681

Madan A (2005) Vibration control of building structures using self-organizing and self-learning neural networks. *Journal of Sound and Vibration*, *287*, 759–784. https://doi.org/10.1016/j.jsv.2004.11.031

Malhis M, Gaudiller L and Hagopian JD (2005) Fuzzy modal active control of flexible structures. *Journal of Vibration and Control*, *11*, 67–88. https://doi.org/10.1177/10775463045046028

Meurers T, Veres SM and Tan ACH (2003) Model-free frequency domain iterative active sound and vibration control. *Control Engineering Practice*, *11*, 1049–1059. https://doi.org/10.1016/S0967-0661(02)00218-6

Parameswaran AP, Pai AB, Tripathi P K, et al. (2013) Active Vibration Control of a Smart Cantilever Beam on General Purpose Operating System. *Defence Science Journal*, 63(4), 413–417. https://doi.org/10.14429/dsj.63.4865

Parameswaran AP, Ananthakrishnan B and Gangadharan KV (2015) Modeling and design of field programmable gate array based real time robust controller for active control of vibrating smart system. *Journal of Sound and Vibration*, 345, 18–33. https://doi.org/10.1016/j.jsv.2015.02.002

Parameswaran AP, Ananthakrishnan B and Gangadharan KV (2015) Design and development of a model free robust controller for active control of dominant flexural modes of vibrations in a smart system. *Journal of Sound and Vibration*, *355*, 1–18. https://doi.org/10.1016/j.jsv.2015.05.006

Parameswaran AP and Gangadharan KV (2015) Parametric modeling and FPGA based

real time active vibration control of a piezoelectric laminate cantilever beam at resonance. *Journal of Vibration and Control*, 21(14), 2881–2895. https://doi.org/10.1177/1077546313518818

Rigatos GG (2009) Model-based and model-free control of flexible-link robots: A comparison between representative methods. *Applied Mathematical Modelling*, *33*, 3906–3925. https://doi.org/10.1016/j.apm.2009.01.012

Swevers J, Lauwerys C, Vandersmissen B, et al. (2007) A model-free control structure for the on-line tuning of the semi-active suspension of a passenger car. *Mechanical Systems and Signal Processing*, *21*, 1422–1436. https://doi.org/10.1016/j.ymssp.2006.05.005

Thenozhi S and Yu W (2015) Active vibration control of building structures using fuzzy proportional-derivative/proportional-integral-derivative control. *Journal of Vibration and Control*, *21*(12), 2340–2359. https://doi.org/10.1177/1077546313509127

Wang J, Jin F, Zhou L, et al. (2019) Implementation of model-free motion control for active suspension systems. *Mechanical Systems and Signal Processing*, *119*, 589–602. https://doi.org/10.1016/j.ymssp.2018.10.004

Wei C, Luo J, Dai H, et al. (2018) Adaptive model-free constrained control of postcapture flexible spacecraft: a Euler–Lagrange approach. *Journal of Vibration and Control*, *24*(20), 4885–4903. https://doi.org/10.1177/1077546317736965

Yang SM, Chen CJ and Huang WL (2006) Structural vibration suppression by a neural-network controller with a mass-damper actuator. *Journal of Vibration and Control*, *12*(5), 495–508. https://doi.org/10.1177/1077546306064269

Yiğit I (2017) Model free sliding mode stabilizing control of a real rotary inverted pendulum. *Journal of Vibration and Control*, *23*(10), 1645–1662. https://doi.org/10.1177/1077546315598031

Yildirim Ş (2004) Vibration control of suspension systems using a proposed neural network. *Journal of Sound and Vibration*, *277*, 1059–1069. https://doi.org/10.1016/j.jsv.2003.09.057

Yonezawa H, Kajiwara I and Yonezawa A (2019) Model-free vibration control to enable vibration suppression of arbitrary structures. In *2019 12th Asian Control Conference, ASCC 2019* (pp. 289–294). JSME.

Yonezawa H, Kajiwara I and Yonezawa A (2020) Experimental verification of model-free active vibration control approach using virtually controlled object. *Journal of Vibration and Control*, (in press). https://doi.org/10.1177/1077546320902348

Yousefi H, Hirvonen M, Handroos H, et al. (2008) Application of neural network in suppressing mechanical vibration of a permanent magnet linear motor. *Control Engineering Practice*, *16*, 787–797. https://doi.org/10.1016/j.conengprac.2007.08.003

Zbou K, Doyle JC and Glover K (1996) *Robust and Optimal Control*. Prentice Hall.

Zhang Q, Wang S, Zhang A, et al. (2017) Improved PI neural network-based tension control for stranded wire helical springs manufacturing. *Control Engineering Practice*, *67*, 31–42. https://doi.org/10.1016/j.conengprac.2017.06.010

Zhou YL, Zhang QZ, Li XD, et al. (2008) On the use of an SPSA-based model-free feedback controller in active noise control for periodic disturbances in a duct. *Journal of Sound and Vibration*, *317*, 456–472. https://doi.org/10.1016/j.jsv.2008.05.027

Figure 1. Proof–mass actuator.

Figure 2. Model for control system design: (a) actual system; (b) system with virtual structure.

Figure 3. Transfer property from x_1 to x_v.

Figure 4. Block diagrams of the control system considering actuator's uncertainty: (a) plant set with feedback-type fluctuation by actuator's parameter uncertainty; (b) generalized plant used to design the H_∞ controller.

Figure 5. Simulation setup.

Figure 6. Frequency response obtained in the simulations: (a) control result with ErK : 0% ErC : 0%; (b) control result with ErK : 50% ErC : −50%.

Figure 7. Experimental system: (a) overview of the controlled object; (b) system diagram; (c) experimental setup.

Figure 8. Frequency response obtained in the experiments (ErK : 0% ErC : 0%).

Figure 9. Frequency response obtained in the experiments (ErK : 50% ErC : 50%).

Figure 10. Frequency response obtained in the experiments (ErK : −50% ErC : 50%).

Figure 11. Frequency response obtained in the experiments (ErK : 50% ErC : −50%).

Figure 12. Frequency response obtained in the experiments (ErK : −50% ErC : −50%).

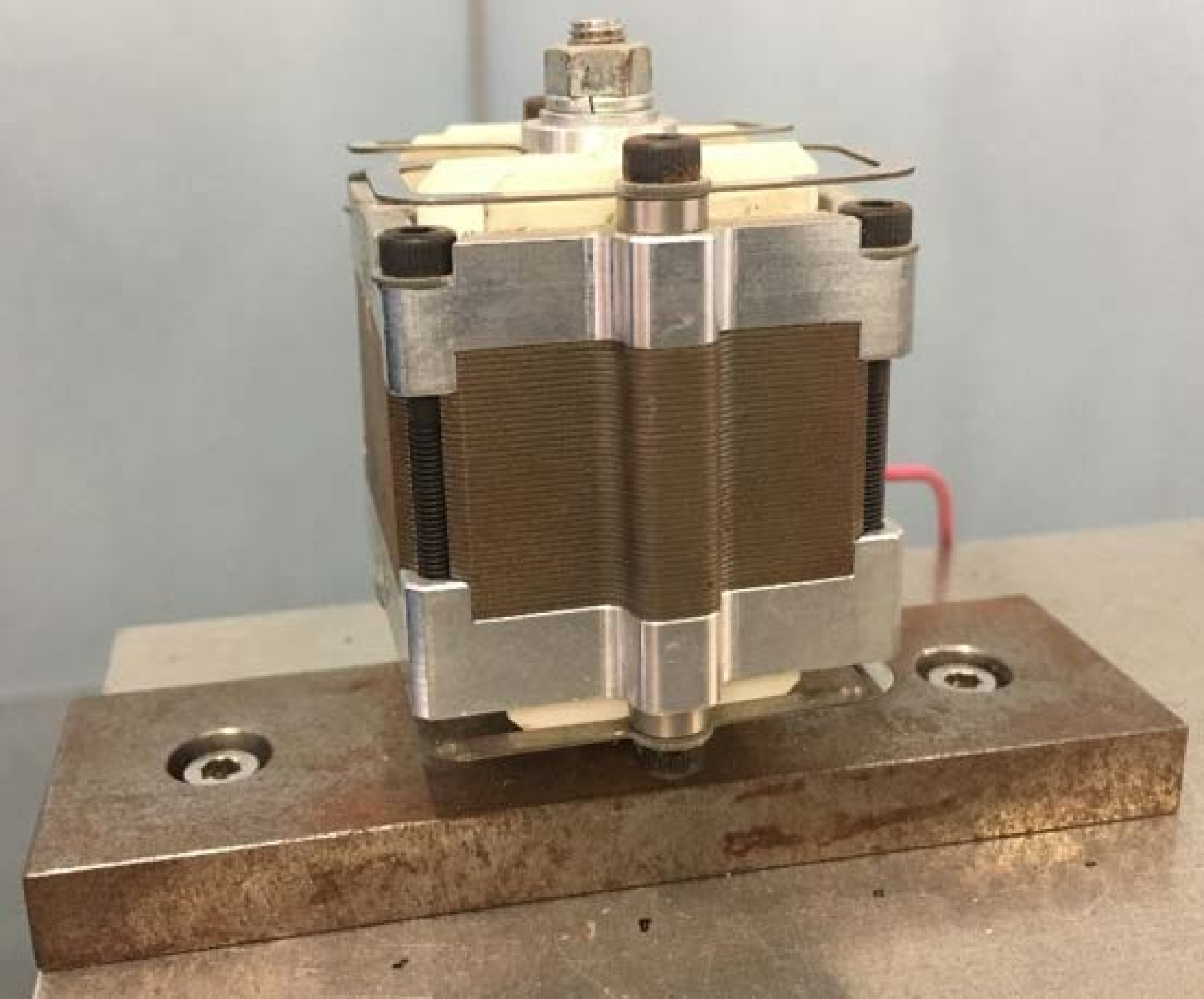

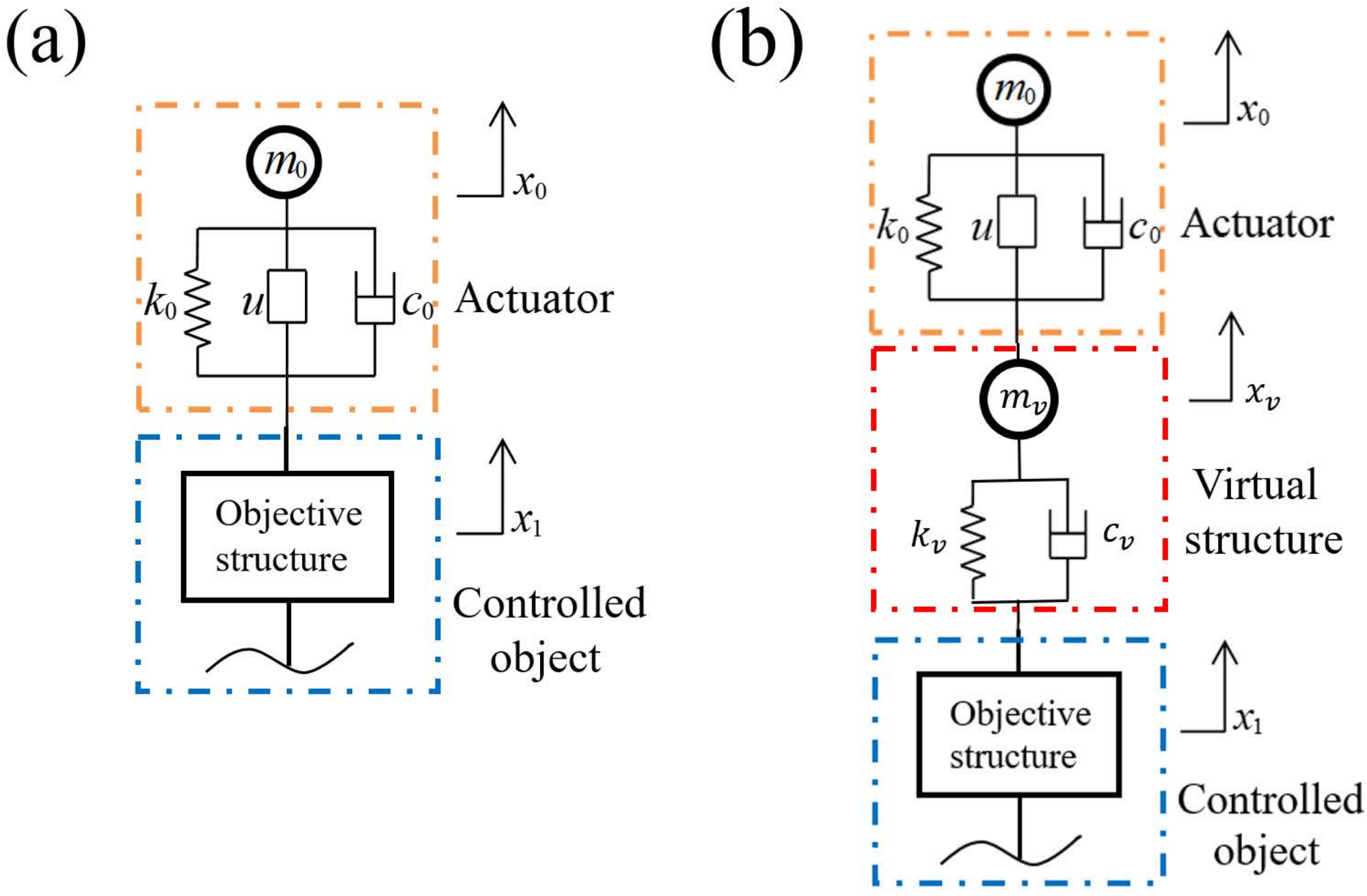
(a)
m_0
x_0
k_0
u
c_0
Actuator
Objective structure
x_1
Controlled object
(b)
m_0
x_0
k_0
u
c_0
Actuator
m_v
x_v
k_v
c_v
Virtual structure
Objective structure
x_1
Controlled object

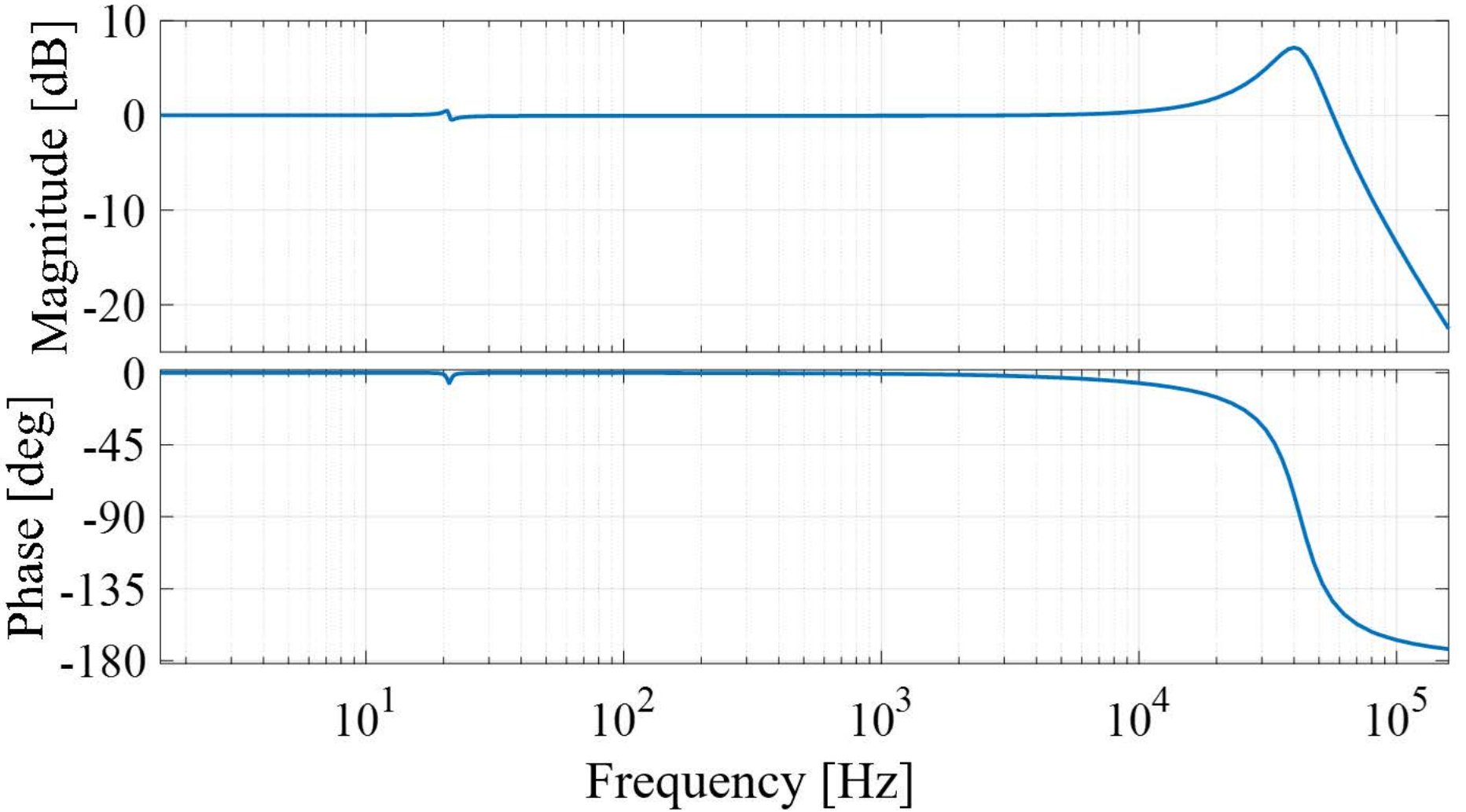
Magnitude [dB]
10
0
-10
-20
Phase [deg]
0
-45
-90
-135
-180
10^1
10^2
10^3
10^4
10^5
Frequency [Hz]

(a)

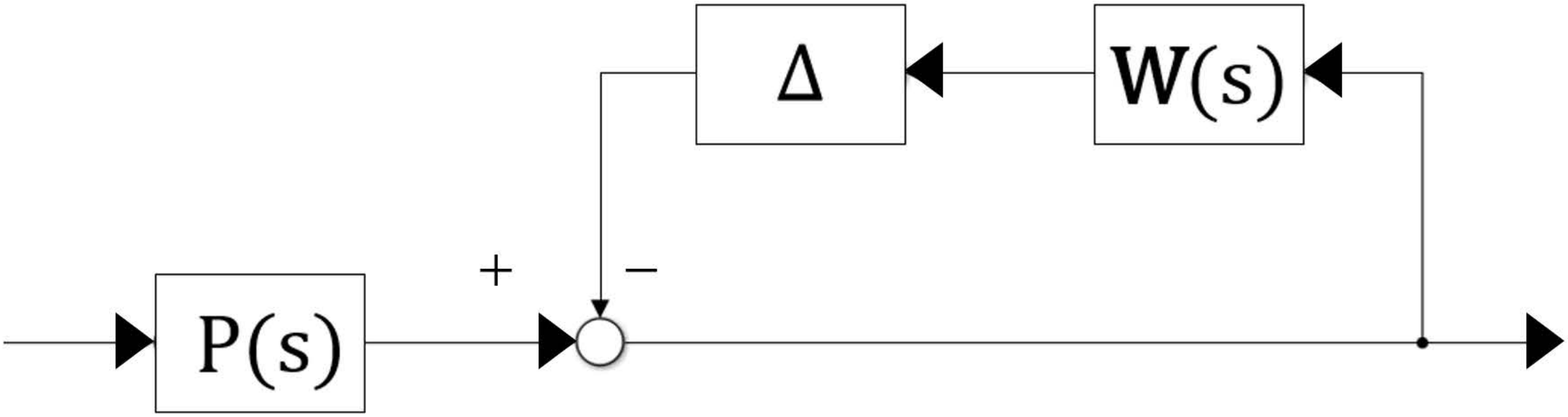

(b)

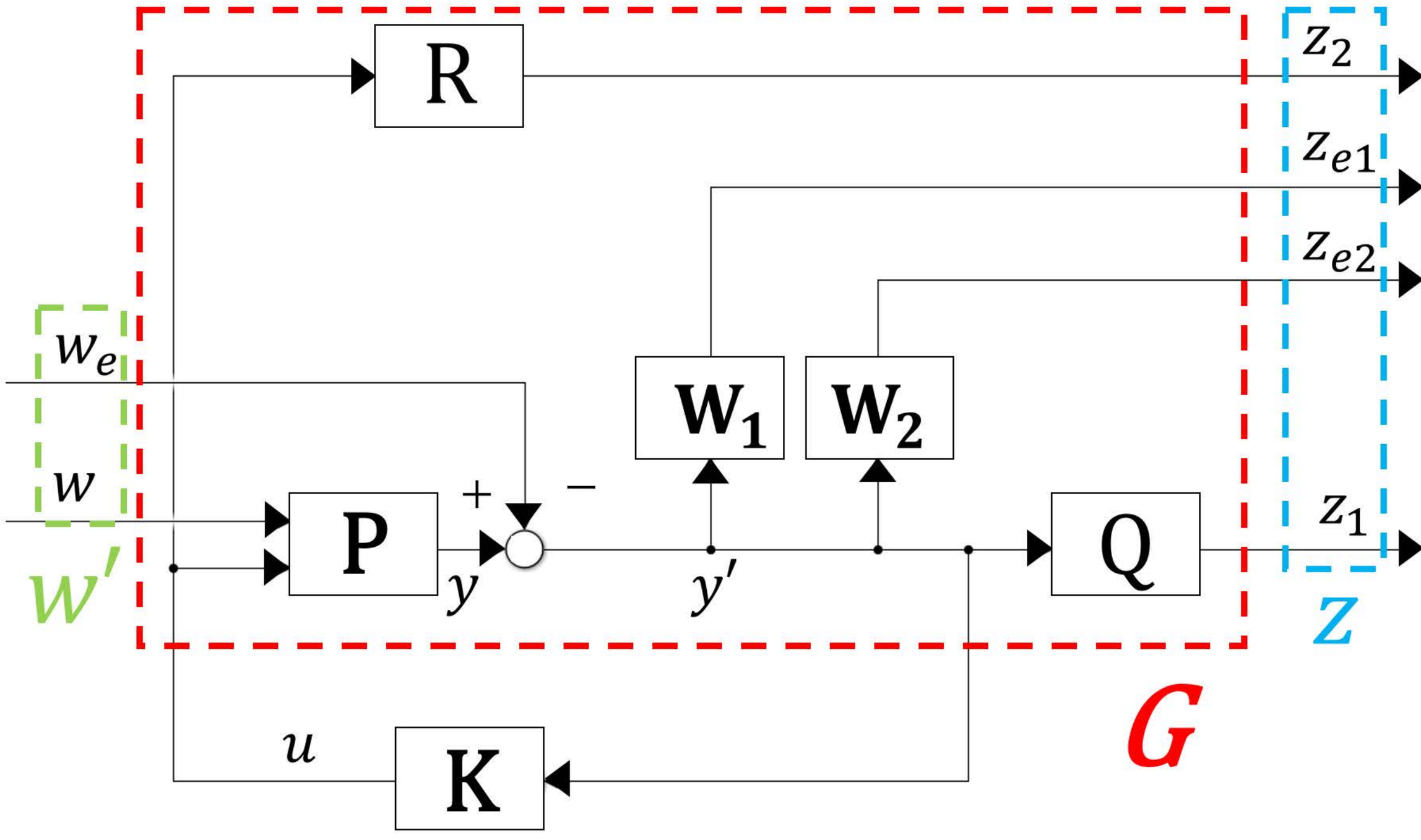

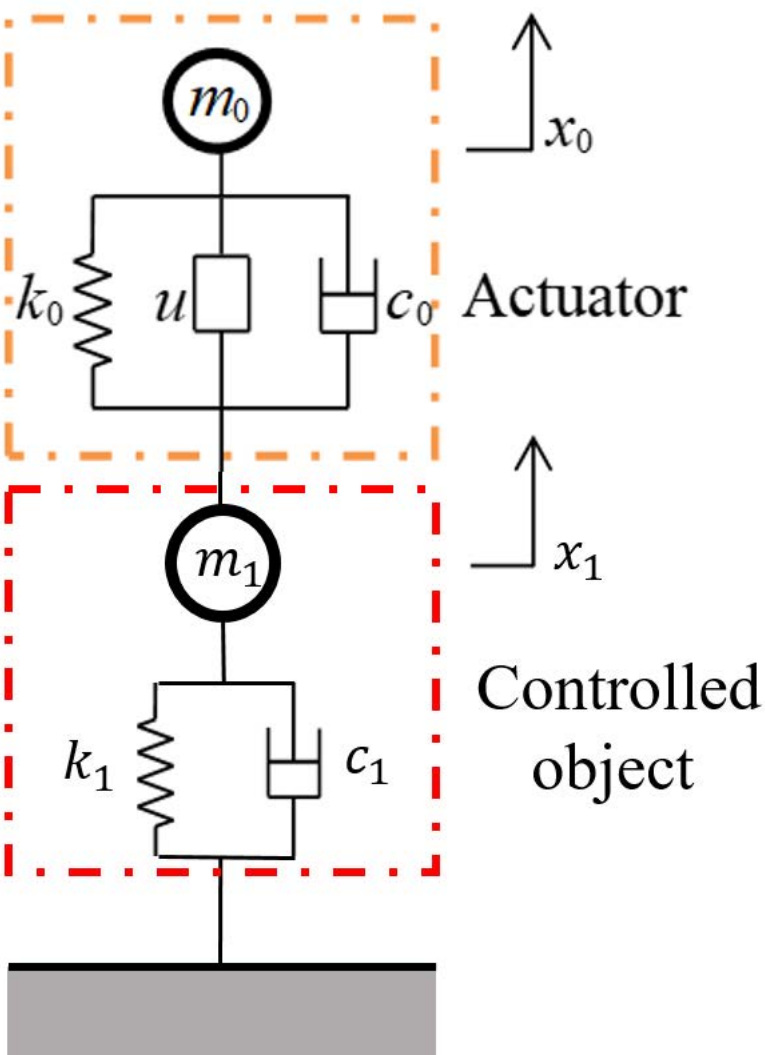
m_0
x_0
k_0
u
c_0
Actuator
m_1
x_1
Controlled object
k_1
c_1

(a)

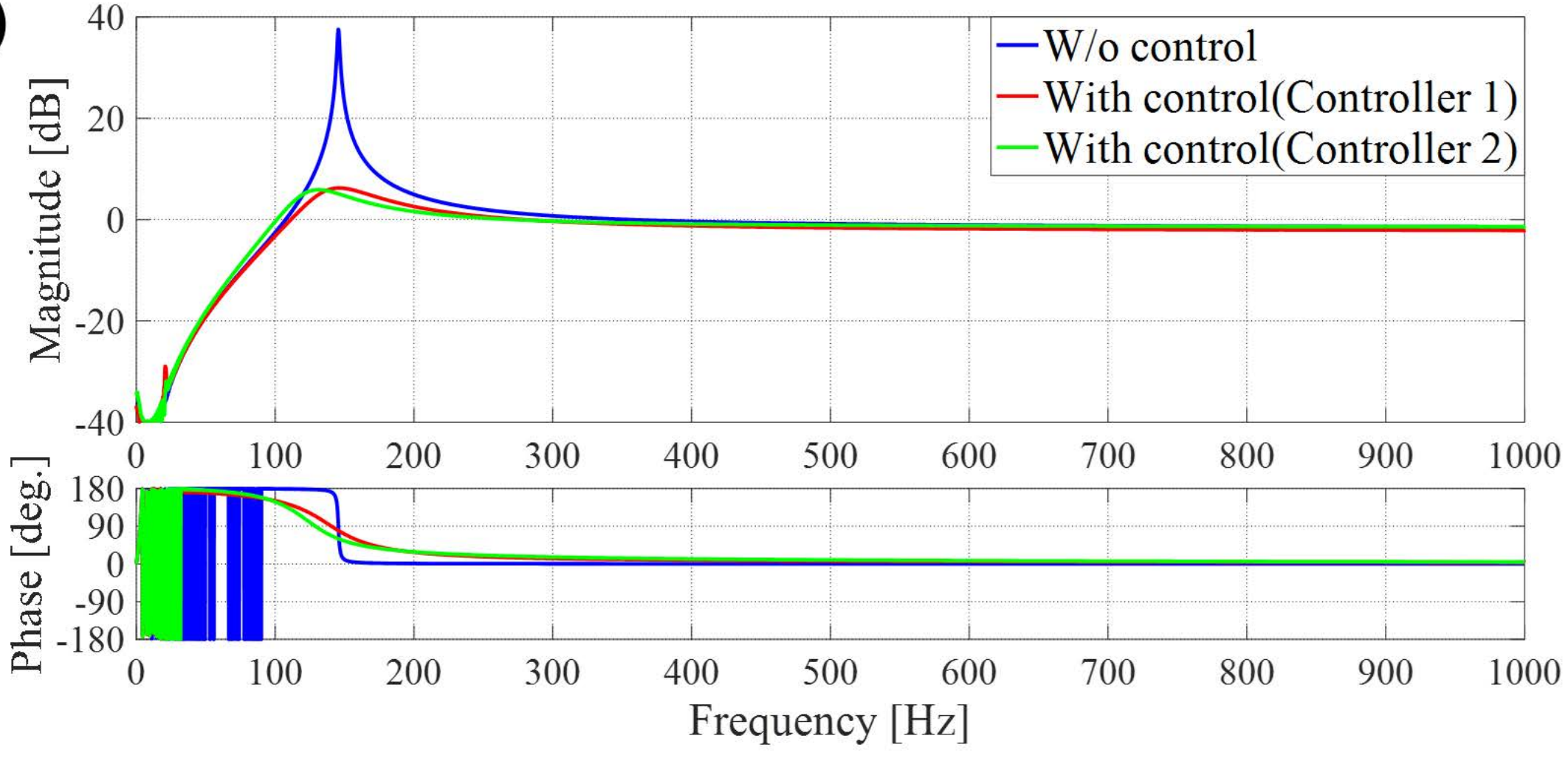
W/o control
With control(Controller 1)
With control(Controller 2)
Magnitude [dB]
Phase [deg.]
Frequency [Hz]
40
20
0
-20
-40
180
90
0
-90
-180
0
100
200
300
400
500
600
700
800
900
1000

(b)

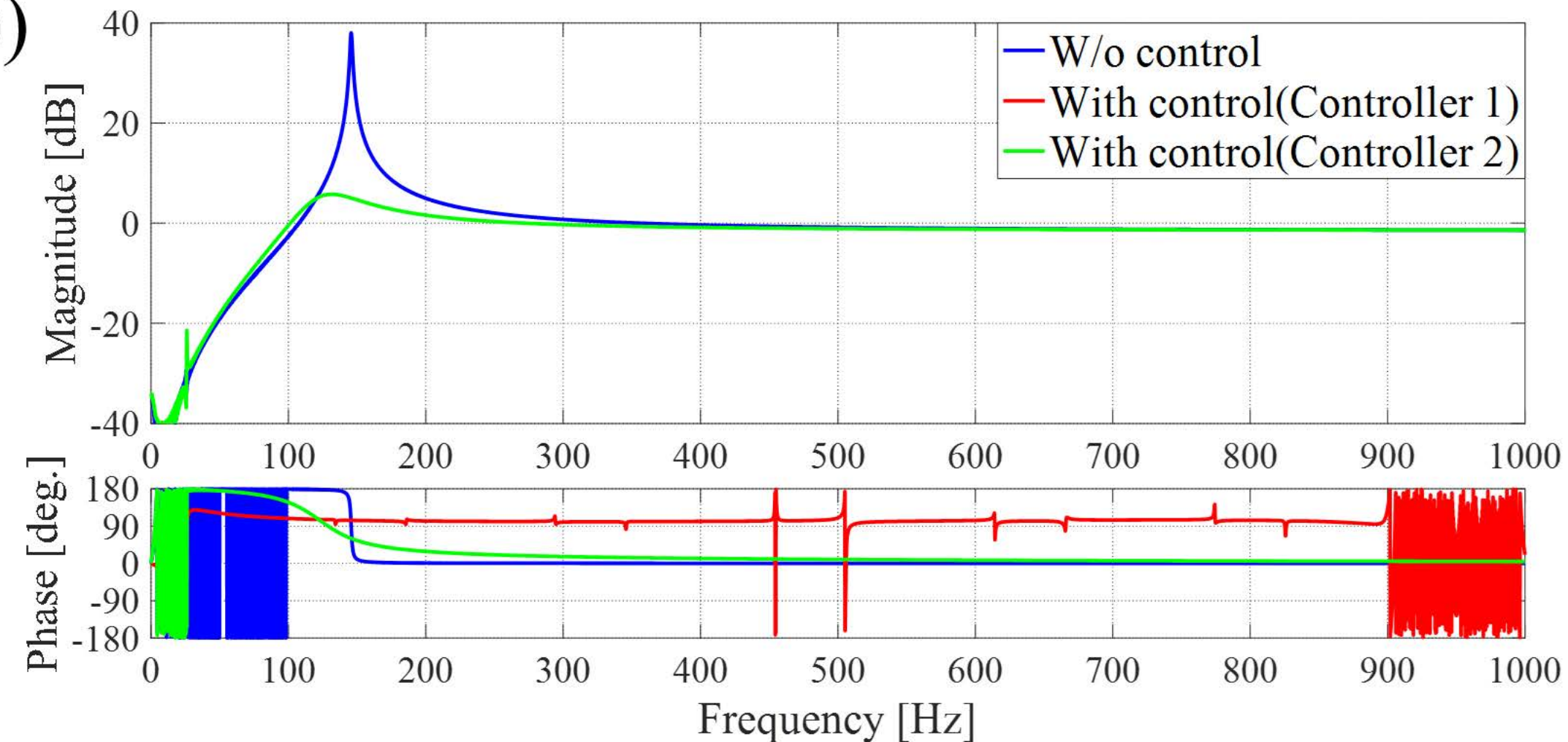
W/o control
With control(Controller 1)
With control(Controller 2)
Magnitude [dB]
Phase [deg.]
Frequency [Hz]
40
20
0
-20
-40
180
90
0
-90
-180
0
100
200
300
400
500
600
700
800
900
1000

(a)

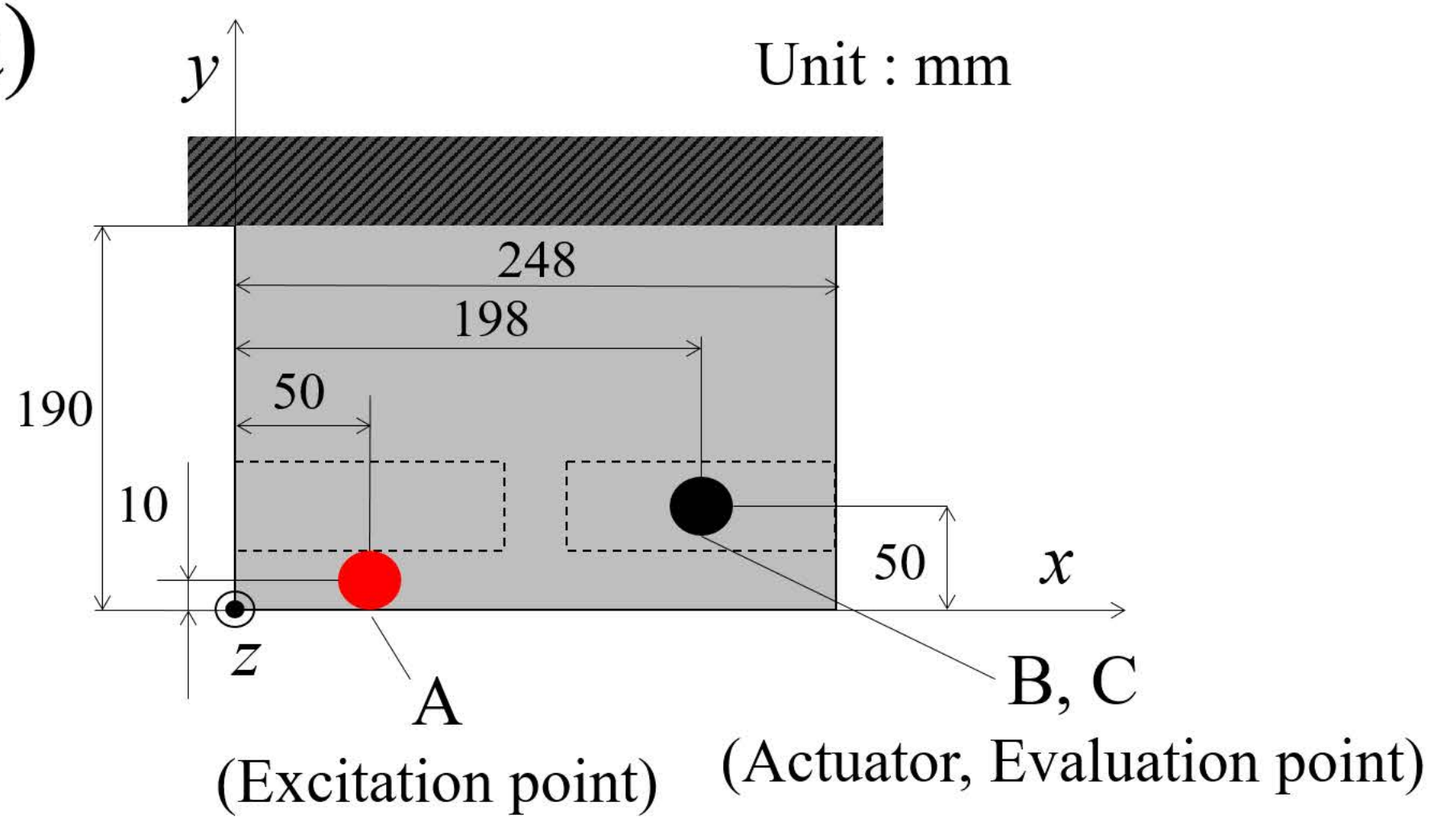
y
Unit : mm
248
198
50
190
10
50
x
z
A
B, C
(Excitation point)
(Actuator, Evaluation point)

(b)

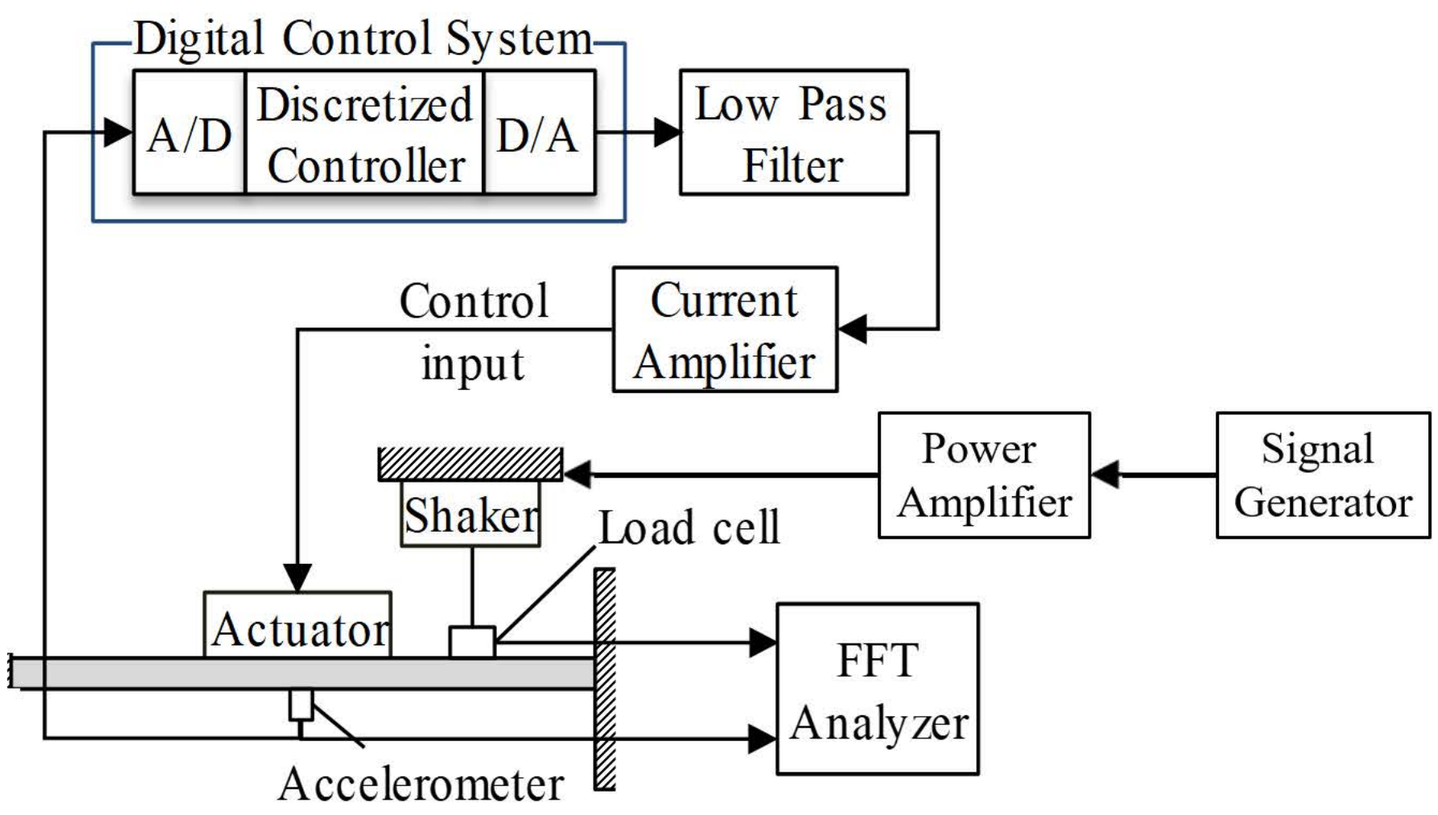
Digital Control System
A/D
Discretized Controller
D/A
Low Pass Filter
Control input
Current Amplifier
Power Amplifier
Signal Generator
Shaker
Load cell
Actuator
FFT Analyzer
Accelerometer

(c)

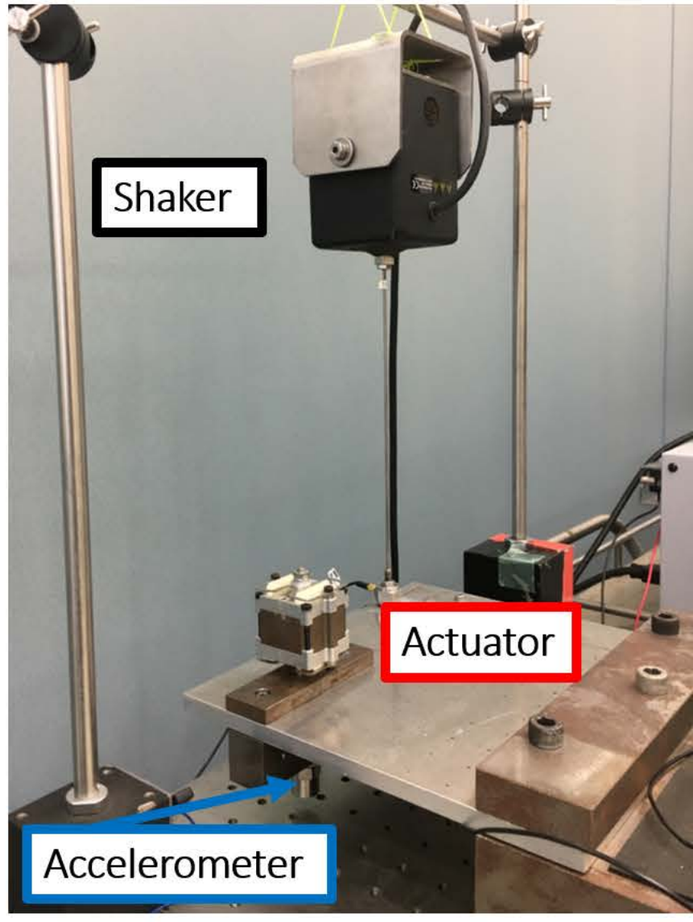
Shaker
Actuator
Accelerometer

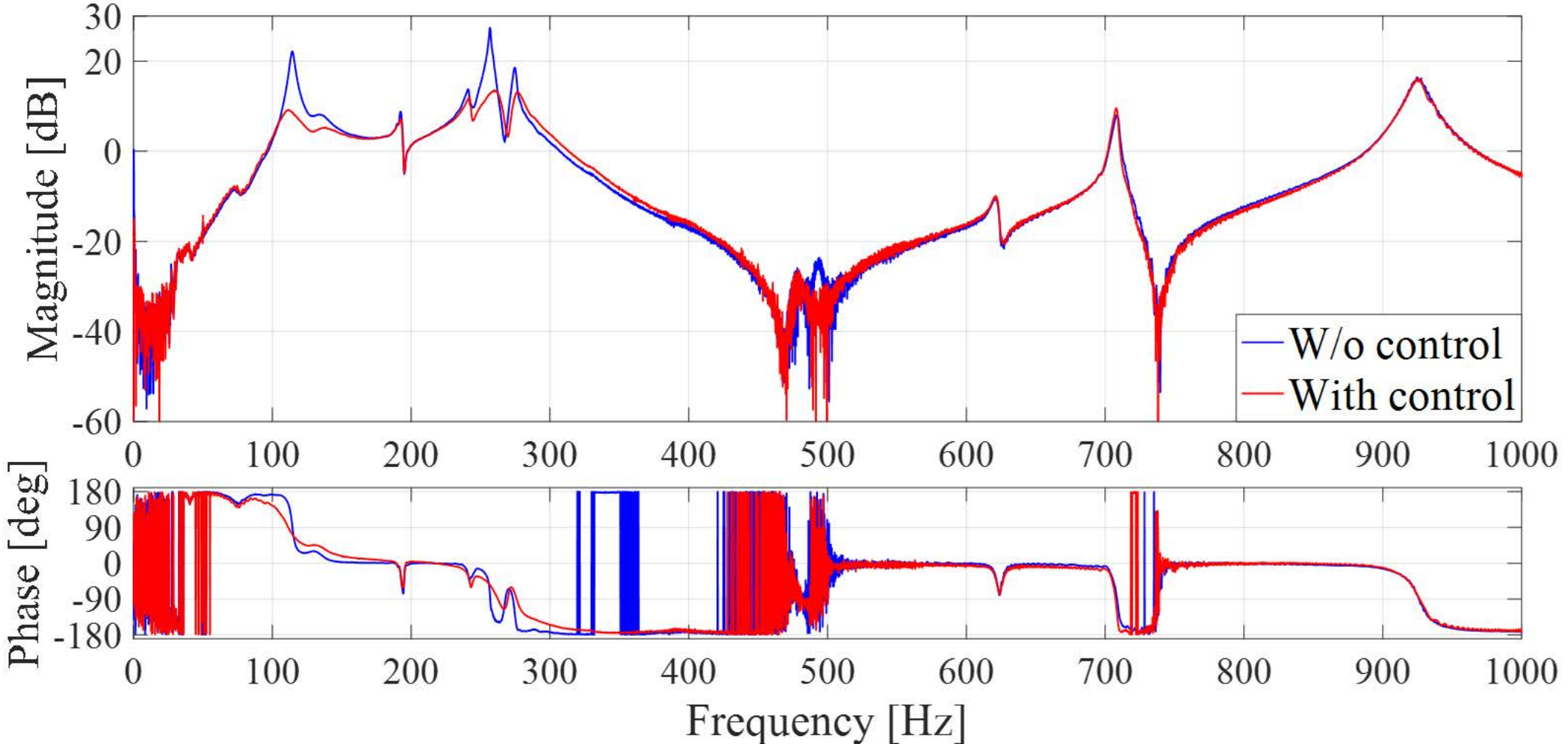
Magnitude [dB]
30
20
0
-20
-40
-60
W/o control
With control
0
100
200
300
400
500
600
700
800
900
1000
Phase [deg]
180
90
0
-90
-180
Frequency [Hz]

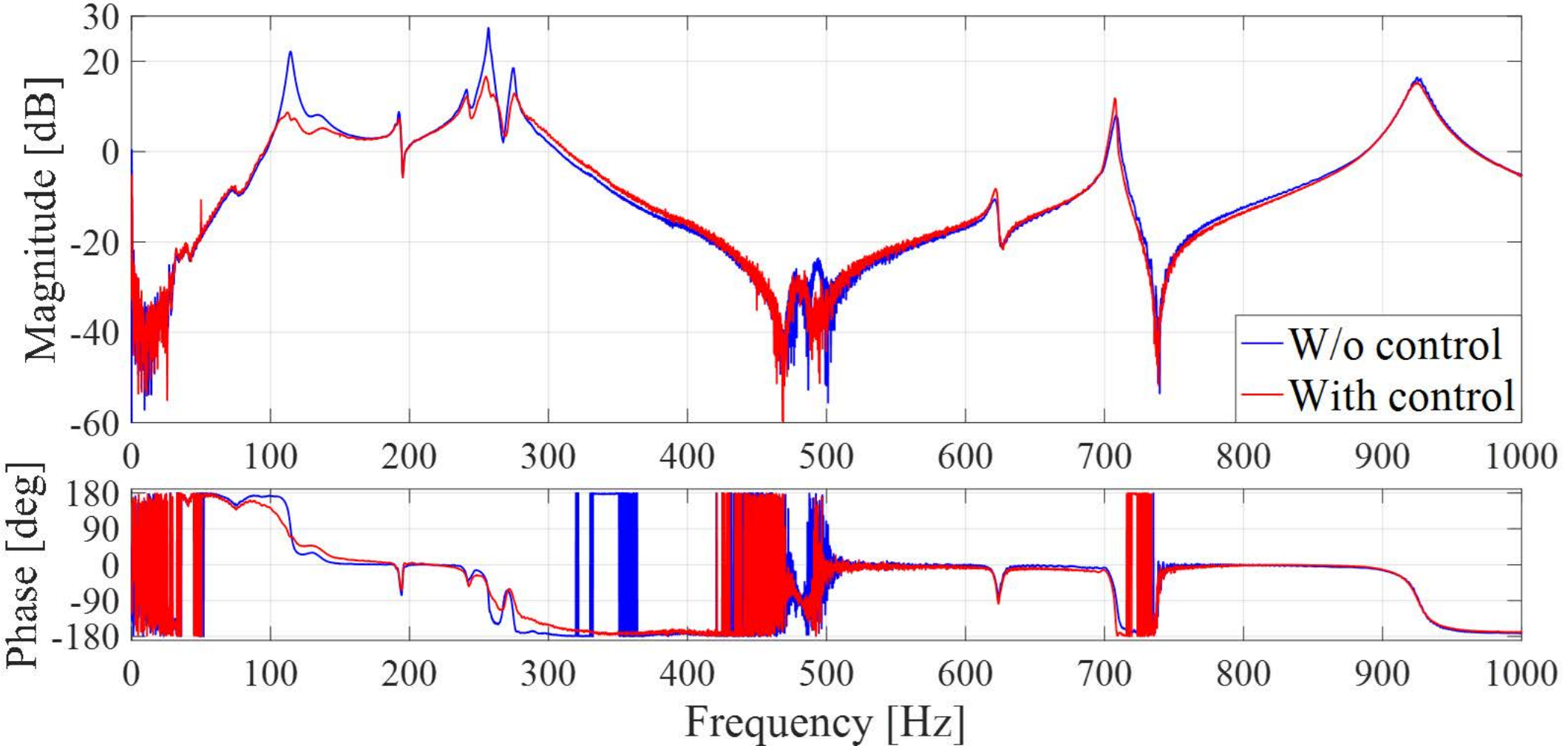
Magnitude [dB]
30
20
0
-20
-40
-60
W/o control
With control
0
100
200
300
400
500
600
700
800
900
1000
Phase [deg]
180
90
0
-90
-180
Frequency [Hz]

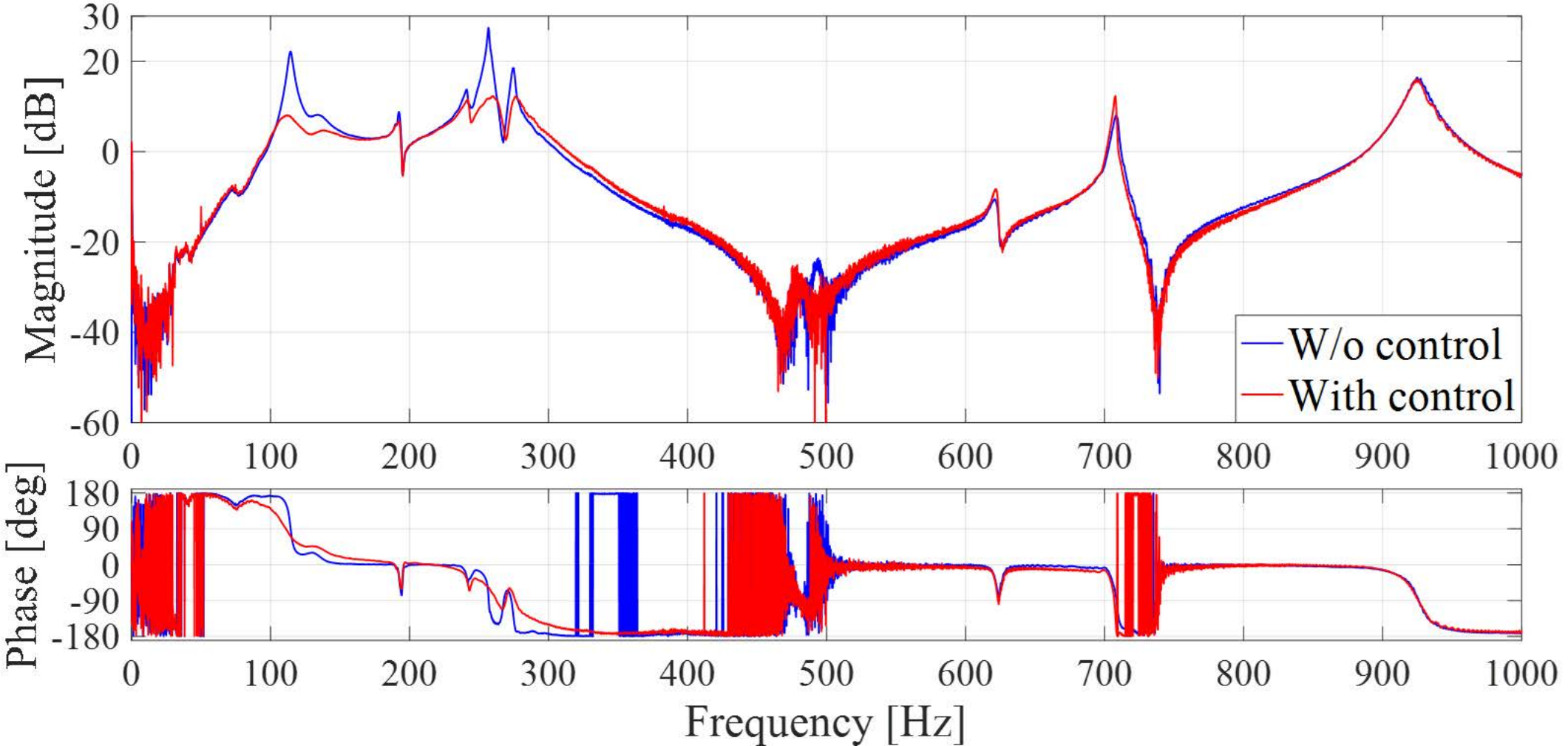
Magnitude [dB]
30
20
0
-20
-40
-60
W/o control
With control
0
100
200
300
400
500
600
700
800
900
1000
Phase [deg]
180
90
0
-90
-180
Frequency [Hz]

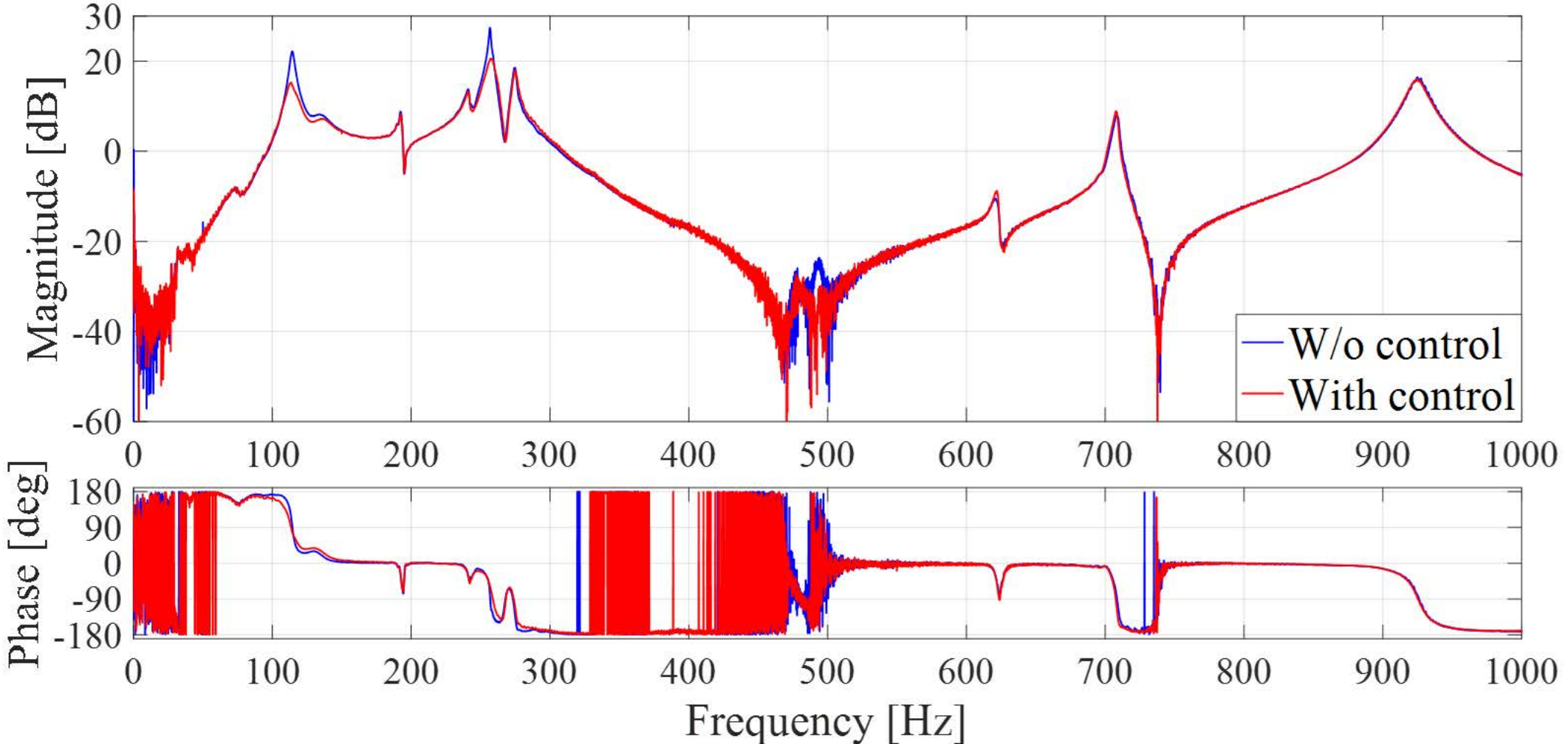
Magnitude [dB]
30
20
0
-20
-40
-60
W/o control
With control
Phase [deg]
180
90
0
-90
-180
0
100
200
300
400
500
600
700
800
900
1000
Frequency [Hz]

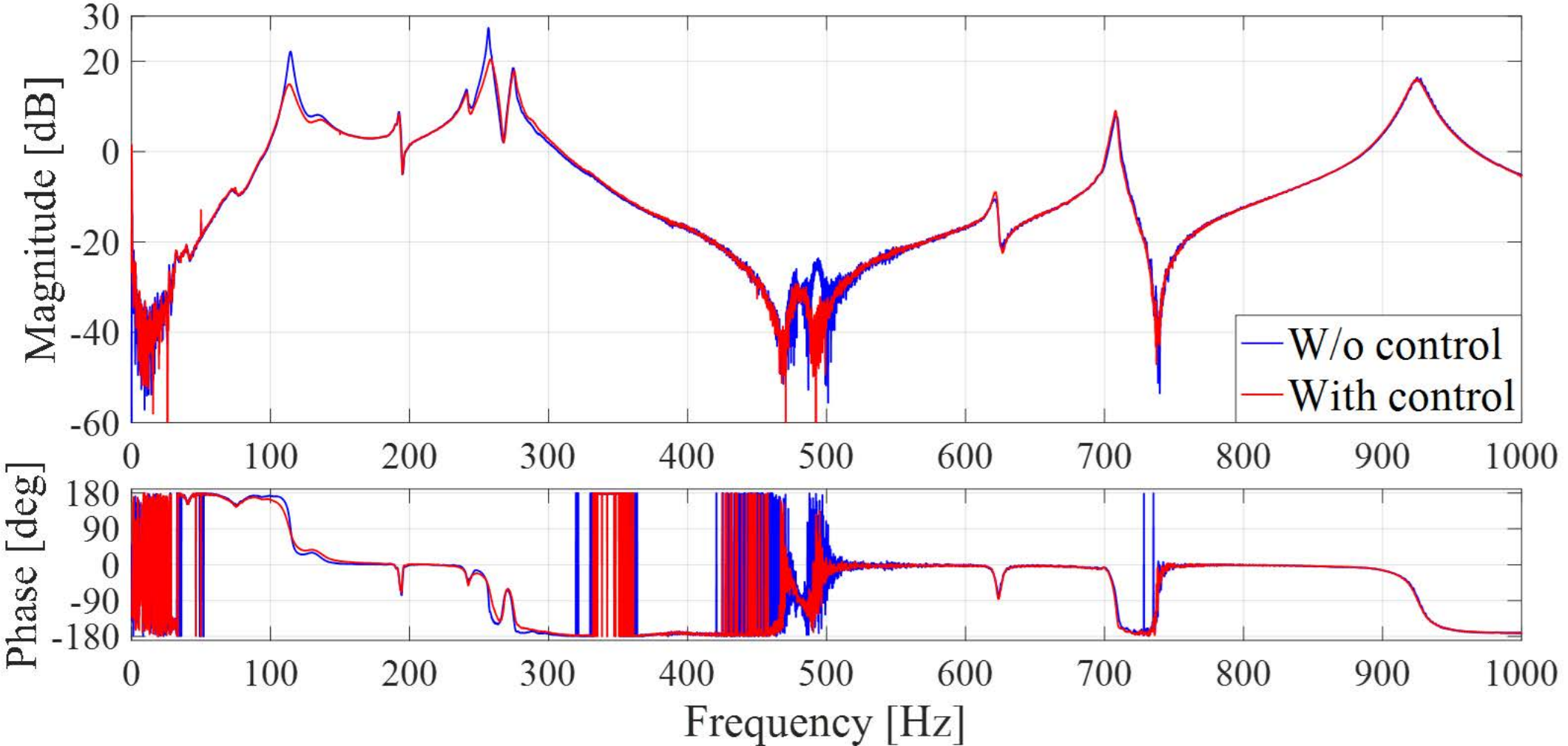
Magnitude [dB]
30
20
0
-20
-40
-60
W/o control
With control
0
100
200
300
400
500
600
700
800
900
1000
Phase [deg]
180
90
0
-90
-180
Frequency [Hz]